



Correlation between the magnetic resonance imaging features of squamous cell carcinoma of the buccal mucosa and pathologic depth of invasion

Akira Baba, MD, PhD,^a Koichi Masuda, MD,^b Kazuhiko Hashimoto, DDS, PhD,^c Satoshi Matsushima, MD, PhD,^a Hideomi Yamauchi, MD, PhD,^a Koshi Ikeda, MD, PhD,^a Masae Yamazaki, DDS,^d Taiki Suzuki, DDS, PhD,^d Satoru Ogane, DDS, PhD,^d Ryo Kurokawa, MD, PhD,^e Mariko Kurokawa, MD,^f Yoshiaki Ota, MD,^g Takuji Mogami, MD, PhD,^b Takeshi Nomura, DDS, PhD,^d and Hiroya Ojiri, MD, PhD^a

Objective. The objective of this study was to determine correlations between magnetic resonance imaging (MRI) features including radiologic depth of invasion (r-DOI) and pathologic DOI (p-DOI) of squamous cell carcinoma of the buccal mucosa.

Study Design. In total, 31 lesions were retrospectively evaluated. MRI findings included detectability, buccinator muscle invasion (positive: BMI+, negative: BMI-), buccal fat pad invasion (positive: BFPI+, negative: BFPI-), and r-DOI measured on T2-weighted images (T2-DOI) and contrast-enhanced T1-weighted images (CET1-DOI). These findings were compared to the p-DOI of the tumors.

Results. The p-DOI values of undetectable lesions were smaller than those of detectable lesions ($P < .001$), and the cutoff value was 1 mm. BMI+ and BFPI+ lesions had significantly larger p-DOI values than the corresponding BMI- and BFPI- lesions ($P < .001$), with cutoff values of 5 and 6 mm, respectively. The correlation coefficient between CET1-DOI and p-DOI was 0.68 ($P < .001$). CET1-DOI values were larger than p-DOI ($P < .001$) and the average difference between them was 3.4 mm. T2-DOI was inconclusive in 50% of cases. Interobserver agreements of MRI evaluation were good to very good.

Conclusion. MRI-derived parameters were useful in estimating p-DOI and may be helpful in predicting the depth of invasion of tumors and the risk of lymph node metastasis. (Oral Surg Oral Med Oral Pathol Oral Radiol 2021;131:582–590)

Squamous cell carcinoma is the most common malignant tumor in the oral cavity; the tongue is the most common location, followed by the mandibular gingiva, the floor of the mouth, the maxillary gingiva, and the buccal mucosa.¹ The eighth edition of the American Joint Committee on Cancer's (AJCC) *Cancer Staging Manual* has added a modification to the tumor classification of cancer in the oral cavity, now incorporating pathologic depth of invasion (p-DOI; Table I).² A strong association exists between p-DOI and lymph node metastasis in the neck, which has been shown to be the most important negative prognostic

factor. An association between p-DOI or tumor thickness and prognosis has also been reported for oral cancer, including carcinoma of the buccal mucosa.^{3,4}

In clinical practice, magnetic resonance imaging (MRI) is widely used for staging malignant diseases of the head and neck, because it is able to detail the extent of tumor invasion. However, the staging manual does not provide a specific description of the radiologic approach for measuring DOI in the preoperative period.² Therefore, it is necessary to standardize an appropriate imaging approach for preoperative radiologic measurements of DOI.

Previous studies regarding tongue cancer have reported a significant correlation between radiologic DOI (r-DOI), as measured by MRI or contrast-enhanced computed tomography, and p-DOI.⁵⁻⁹ In addition, some reports show characteristic MRI findings of oral tongue cancer, including lesion detectability and invasion of the styloglossus and hyoglossus muscles, that are associated with p-DOI values.^{5,6}

However, there are no reports in which MRI findings including r-DOI have been used to estimate p-DOI for

^aDepartment of Radiology, The Jikei University School of Medicine, Minato-ku, Tokyo, Japan.

^bDepartment of Radiology, Tokyo Dental College Ichikawa General Hospital, Ichikawa-shi, Chiba, Japan.

^cDepartment of Pathology and Laboratory Medicine, Tokyo Dental College Ichikawa General Hospital, Ichikawa-shi, Chiba, Japan.

^dOral Cancer Center, Tokyo Dental College, Ichikawa-shi, Chiba, Japan.

^eDepartment of Radiology, Graduate School of Medicine, The University of Tokyo, Bunkyo-ku, Tokyo, Japan.

^fDepartment of Radiology, Tokyo Metropolitan Cancer and Infectious Diseases Center Komagome Hospital, Bunkyo-ku, Tokyo, Japan.

^gDepartment of Radiology, University of Michigan, Ann Arbor, MI, USA.

Received for publication Sep 18, 2020; returned for revision Dec 24, 2020; accepted for publication Dec 31, 2020.

© 2021 Elsevier Inc. All rights reserved.

2212-4403/\$-see front matter

<https://doi.org/10.1016/j.oooo.2020.12.023>

Statement of Clinical Relevance

Magnetic resonance imaging parameters of buccal mucosa squamous cell carcinoma can be helpful in predicting the pathologic depth of invasion of tumors, which can assist in estimating the tumor stage and risk of metastasis of the lesions.

Table 1. Tumor categorization of oral cavity cancer in the American Joint Committee on Cancer’s *Cancer Staging Manual*, eighth edition

T1	Tumor ≤ 2 cm with DOI ≤ 5 mm
T2	Tumor ≤ 2 cm with DOI > 5 mm
	Tumor > 2 cm and ≤ 4 cm with DOI ≤ 10 mm
T3	Tumor > 2 cm and ≤ 4 cm with DOI > 10 mm
	Tumor > 4 cm, DOI ≤ 10 mm
T4a	Tumor > 4 cm with DOI > 10 mm
	Tumor invades adjacent structures only (e.g., through cortical bone of the mandible/maxilla or involves the maxillary sinus or skin of the face)
T4b	Tumor invades the masticator space, pterygoid plates, or skull base and/or encases the internal carotid artery

DOI, depth of invasion.

squamous cell carcinoma of the buccal mucosa (SCCBM). Anatomic features of the buccinator muscle located beneath the buccal mucosa and the buccal fat pad located beneath the buccinator muscle (Figure 1) are similar to the relationship of the stylohyoid and hyoglossus muscles and tongue mucosa. Therefore, we hypothesized that MRI detectability, MRI findings (buccinator muscle invasion [BMI] and buccal fat pad invasion [BFPI]), and MRI r-DOI measurements might be associated with p-DOI for SCCBM and can be used for its estimation. The objective of the study was to evaluate the correlations between MRI features of SCCBM and pathologic p-DOI. The null hypothesis stated that there would be no statistically significant correlations between the MRI parameters and the pathologic measurements of DOI.

MATERIALS AND METHODS

Patients

We retrospectively evaluated consecutive patients who underwent radical surgery for primary SCCBM and who underwent MRI for pretreatment evaluation between April 2011 and April 2020. This retrospective study was

approved by the institutional review board and ethics committee at our institution. The requirement of informed consent was waived because the study was retrospective in nature. All procedures were performed in accordance with the ethical standards of the responsible committees on human experimentation (institutional and national) and with the Declaration of Helsinki of 1975 (revised in 2008).

Acquisition of MRI scans

MRI was performed on an Achieva 1.5-T system (Philips Medical Systems, Amsterdam, The Netherlands) using a maximum gradient field strength of 33 mT/m and a 2-channel Flex S coil, and on an Ingenia 3.0-T system (Philips Medical Systems) using a maximum gradient field strength of 45 mT/m and a head coil. All patients were examined in the supine position. Each field of view (FOV) was set to the maxillofacial region.

Axial T2-weighted images were obtained using the following parameters: repetition time (TR)/echo time (TE) 2800 to 3000 ms/84 to 90 ms; flip angle 90°; FOV 15 to 18 × 15 to 18 cm; matrix size 288 × 222 to 230; slice thickness 3.5 to 4 mm; gap 0.3 to 0.4 mm; number of excitations (NEX) 1 to 2. Coronal T2-weighted images were obtained using the following parameters: TR/TE 3000 to 4300 ms/84 to 90 ms; flip angle 90°; FOV 15 to 18 × 15 to 18 cm; matrix size 288 × 214 to 230; slice thickness 3.5 to 4 mm; gap 0.3 to 0.4 mm; NEX 1 to 2. Coronal contrast-enhanced fat-suppressed T1-weighted images (CET1) were obtained using the following parameters: TR/TE 550 ms/10 ms; flip angle 90°; FOV 15 × 15 cm; matrix size 320 × 256; slice thickness 3.5 mm; gap 0.3 mm; NEX 2. Coronal contrast-enhanced fat-suppressed T1-weighted images (mDIXON water images) were obtained using the following parameters: TR/TE1/TE2 (shortest) 6 ms/(shortest) 2 ms/(shortest) 3 ms; flip angle 15°; FOV 20 × 20 cm; matrix size 192 × 190; slice thickness 1.1 mm; gap 0.55 mm; NEX 1.

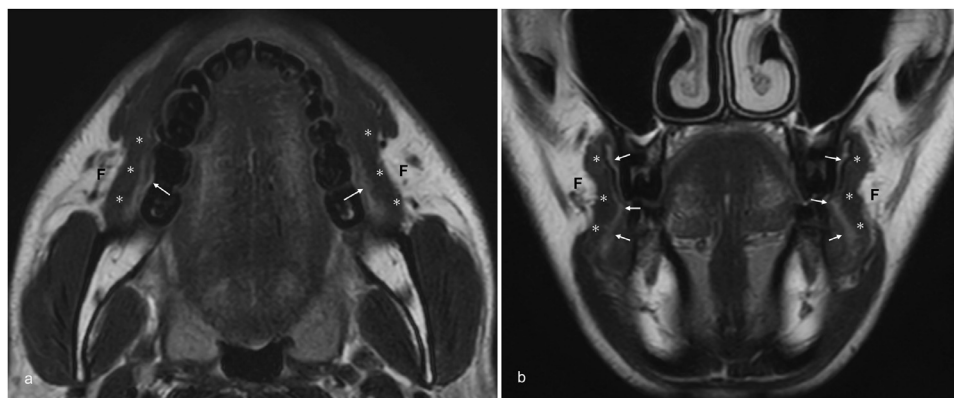


Fig. 1. Normal anatomy of the buccal mucosa, buccinator muscle, and buccal fat pad. A 35-year-old male. (a) Axial and (b) coronal T2-weighted images show normal buccal mucosa (arrows), buccinator muscle (*), and buccal fat pad (F).

Evaluation of MRI scans

MRI findings were evaluated for detectability of lesions, presence of BMI, and presence of BFPI. The tumors were considered to be detectable lesions (DLs) if they were detected on axial and coronal T2-weighted or coronal CET1-weighted imaging. They were classified as undetectable lesions (ULs) if they could not be detected on any MRI sequences (Figure 2). BMI was determined to be positive (BMI+) when the buccinator muscle, which normally appears as a low signal intensity, was obscured by tumor invasion in axial and coronal T2-weighted imaging, and negative (BMI-) was determined in the absence of these features (Figure 3). ULs were classified as BMI-. BFPI was determined to be positive (BFPI+) when the buccinator muscle was obscured in all layers with tumor invasion of the adjacent buccal fat pad on axial and coronal T2-weighted imaging, and negative (BFPI-) when there was no evidence of invasion (Figure 4). ULs were classified as BFPI-. r-DOI was measured from the horizon reference line, determined as the line connecting the junctions of the tumor and the normal mucosa on both sides, to the deepest aspect of the tumor as detected in coronal T2-weighted imaging (T2-DOI) and coronal contrast-enhanced fat-suppressed T1-weighted imaging (CET1-DOI; Figure 5a).^{5-9,22} Protruding and/or ulcerative portions of the lesion were ignored.²² This measurement method was implemented in the same manner as specified by the p-DOI measurement protocol of the *AJCC Cancer Staging Manual*, eighth edition,² for pathologic sections as described below.

Two board-certified radiologists with 11 and 8 years of experience, respectively, retrospectively evaluated MRI findings and r-DOI of SCCBM in all patients independently and blindly without knowing the pathologic results. The location of lesions and the direction and depth of tumor invasion were determined on the coronal images. If

the 2 observers provided the same interpretation, that result was adopted. If the interpretation differed, the observers came to a consensus decision. A single consensus data set was compiled from these observations and used for statistical analysis. The values of r-DOI calculated from T2-DOI and CET1-DOI that were used in statistical analysis were the average values of the measurements by the 2 radiologists. A picture archiving and communication system (Synapse Viewer, Fuji Medical Systems, Tokyo, Japan) was used by the observers to view and evaluate the scans digitally.

Evaluation of pathologic tissue specimens

Tissue samples from specimens resected in the coronal plane were subjected to pathologic analysis. They were fixed in 10% neutral buffered formalin, embedded, sectioned, and stained with hematoxylin and eosin. The sliced specimens were evaluated by an oral pathologist specializing in oral cancer pathology. p-DOI was measured according to the *AJCC Cancer Staging Manual*, eighth edition,² including descriptions that "DOI is measured by first finding the 'horizon' of the basement membrane of the adjacent squamous mucosa. A perpendicular 'plumb line' is established from this horizon to the deepest point of tumor invasion" (Figure 5b).

Statistical analysis

The Shapiro-Wilk test revealed a nonnormal distribution of data in comparisons between the p-DOI of DL and UL, BMI+ and BMI-, and BFPI+ and BFPI-. The Mann-Whitney *U* test was used to measure the significance of differences between these pairs of values. The cutoff values of the p-DOI between DL and UL, between BMI+ and BMI-, and between BFPI+ and BFPI- were calculated by using the Youden index from the receiver operating characteristic curve.

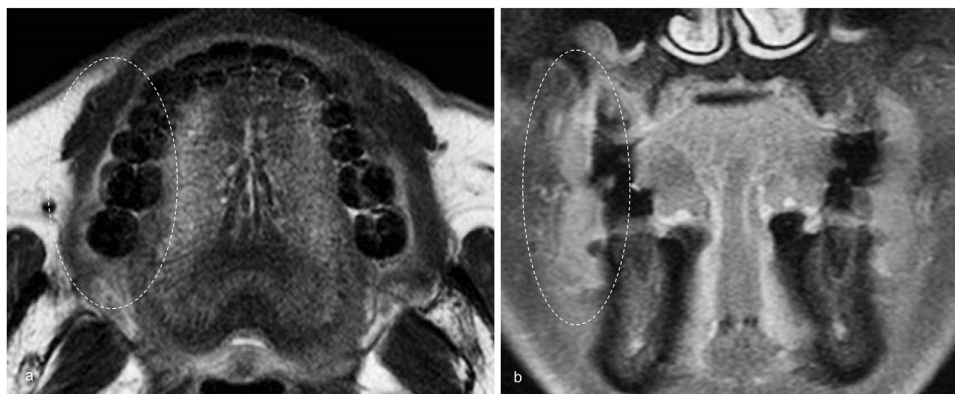


Fig. 2. Undetectable lesion of squamous cell carcinoma of the buccal mucosa (SCCBM) on magnetic resonance imaging. A 70-year-old male with SCCBM on the right side. Neither the (a) axial T2-weighted image nor the (b) coronal contrast-enhanced fat-suppressed T1-weighted coronal image reveal the lesion in the right buccal mucosa (within dotted circle), in which SCCBM was proven clinically and pathologically.

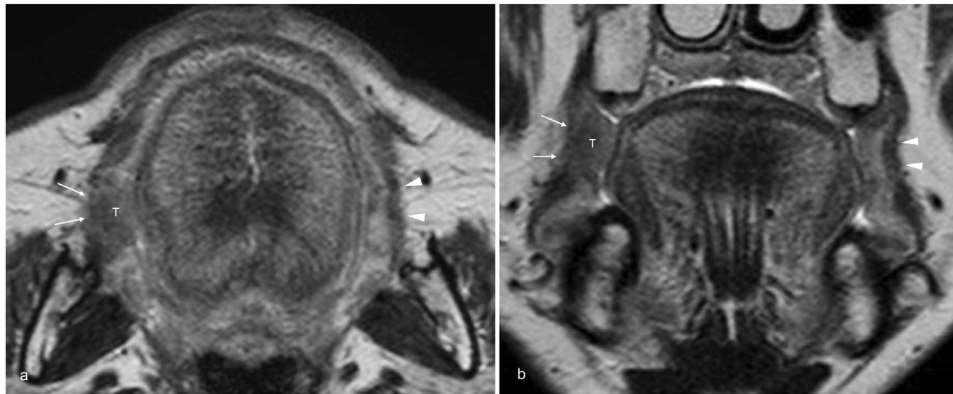


Fig. 3. Magnetic resonance imaging findings of buccinator muscle invasion. A 76-year-old male with squamous cell carcinoma of the right buccal mucosa. (a) Axial and (b) coronal T2-weighted images reveal squamous cell carcinoma of the buccal mucosa (T) with invasion into the right buccinator muscle (arrows). The left buccinator muscle (arrowheads) is normal.

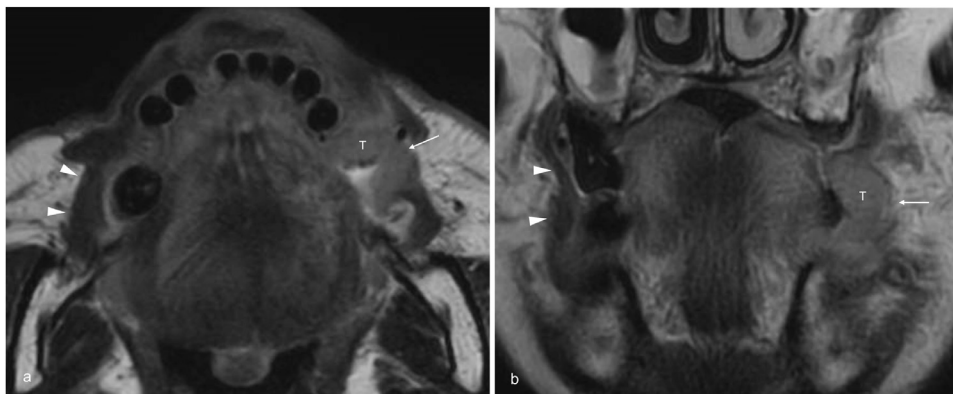


Fig. 4. Magnetic resonance imaging findings of buccal fat pad invasion. A 66-year-old male with squamous cell carcinoma of the left buccal mucosa. (a) Axial and (b) coronal T2-weighted images reveal squamous cell carcinoma of the buccal mucosa (T) with invasion through the buccinator muscle into the left buccal fat pad (arrow). The right buccinator muscle (arrowheads) is normal.

Data were normally distributed for comparisons between T2-DOI and p-DOI and between CET1-DOI and p-DOI. The paired *t* test was used for analysis of these data.

The Spearman test was used to evaluate the correlation of p-DOI with T2-DOI and with CET1-DOI. A *P* value less than .05 was considered to indicate statistical significance.

Interobserver agreement in evaluation of detectability, BMI, and BFPI on MRI was assessed by kappa statistics. A value of 0 to 0.20 indicated poor agreement, 0.21 to 0.40 indicated fair agreement, 0.41 to 0.60 indicated moderate agreement, 0.61 to 0.80 indicated good agreement, and 0.81 to 1.00 indicated very good agreement.¹⁰

All statistical analyses were performed by using R version 3.6.1 (R Foundation for Statistical Computing, Vienna, Austria).

RESULTS

In total, the observers evaluated 31 SCCBM lesions in 31 patients (26 males and 5 females; age range, 56-91 years; average age [\pm SD], 73.3 \pm 8.3 years).

The tumor staging category ranged from T1 to T4a. T2 lesions were most prevalent (12/31, 38.7%), followed by T3 lesions (9/31, 29.0%), T1 lesions (6/31, 19.4%), and T4a lesions (4/31, 12.9%) as classified by the AJCC *Cancer Staging Manual*, eighth edition.² The mean p-DOI of all cases was 5.6 mm (SD = 4.2 mm) and the median was 5.0 mm (range, 0.5–16 mm).

The status of DL and UL was determined in 24 (77.4%) and 7 (22.6%) cases, respectively, based on consensus of the observers. In univariate analysis with the Mann-Whitney *U* test, p-DOI of UL (median, 1 mm; range, 0.5-3.0 mm) was smaller than that of DL (median, 6.0 mm; range, 6.0-16.0 mm; *P* < .001). The cutoff value of p-DOI between DL and UL was 1 mm (Table II).

The status of BMI+ and BMI- was determined in 20 (64.5%) and 11 (35.5%) cases, respectively, as per the observers' consensus. In univariate analysis with the Mann-Whitney *U* test, p-DOI of BMI+ lesions (median, 7.3 mm; range, 0.5-16.0 mm) was larger than that of BMI- lesions (median, 1.5 mm; range, 0.5-4.0 mm;

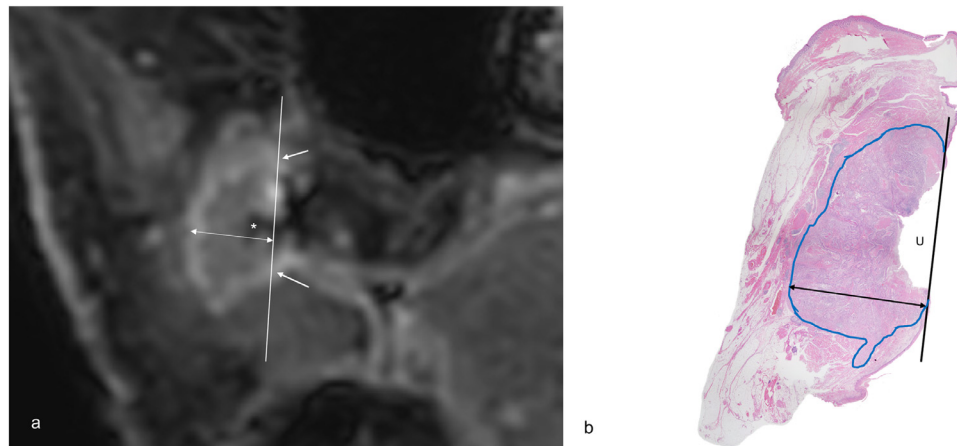


Fig. 5. Measuring radiologic depth of invasion on a contrast-enhanced fat-suppressed T1-weighted image and pathologic depth of invasion on a tissue specimen. An 81-year-old male with squamous cell carcinoma of the right buccal mucosa. (a) Coronal contrast-enhanced T1-weighted image reveals squamous cell carcinoma, with ulcer formation (*), of the right buccal mucosa. Radiologic depth of invasion calculated on the coronal contrast-enhanced T1-weighted image, shown by the 2-directional arrow, is measured from the horizon reference line (solid line), determined as the line connecting the junctions (arrows) of the tumor and normal mucosa, to the deepest aspect of tumor invasion. (b) A hematoxylin and eosin–stained image of the pathologic specimen shows the lesion with ulcer formation (U). Pathologic depth of invasion (2-directional arrow) is measured from the horizon reference line (solid line), connecting the basement membrane of the adjacent normal squamous mucosa, to the deepest aspect of tumor invasion. Radiographic depth of invasion on the contrast-enhanced T1-weighted image was 11 mm and pathologic depth of invasion was 10.2 mm.

Table II. p-DOI values based on detectability, buccinator muscle invasion, and buccal fat pad invasion

	No. of cases	Median (mm)	Range (mm)	P value	Cutoff value (mm)
DL	24 (77.4%)	6	6-16	<.001	1
UL	7 (22.6%)	1	0.5-3		
BMI+	20 (64.5%)	7.3	0.5-16	<.001	5
BMI–	11 (35.5%)	1.5	0.5-4		
BFPI+	10 (32.3%)	10.5	6-16	<.001	6
BFPI–	21 (67.7%)	2	0.5-11		

p-DOI, depth of invasion measured on pathologic specimens; DL, detectable lesions; UL, undetectable lesions; BMI+, lesions with invasion of the buccinator muscle; BMI–, lesions without invasion of the buccinator muscle; BFPI+, lesions with invasion of the buccal fat pad; BFPI–, lesions without invasion of the buccal fat pad.

$P < .001$). The cutoff value of p-DOI between BMI+ and BMI– was 5 mm (Table II).

The status of BFPI+ and BFPI– was determined in 10 (32.3%) and 21 (67.7%) cases, respectively, based on the observers’ consensus. In univariate analysis with the Mann-Whitney test, p-DOI of BFPI+ lesions (median, 10.5 mm; range, 6.0-16.0 mm) was larger than that of BFPI– lesions (median, 2.0 mm; range, 0.5-11.0 mm; $P < .001$). The cutoff value of p-DOI between BFPI+ and BFPI– was 6 mm (Table II).

T2-DOI could not depict the lesions in 12 of 24 cases (50%) because the lack of clear contrast between the adjacent normal mucosa and tumor obscured detailed localization. However, the

Table III. Number of cases classified by the degree of DOI

Range of DOI (mm)	T2-DOI (n = 12)	CET1-DOI (n = 24)	p-DOI (n = 31)
<4	0	0	13
≥4 and ≤5	0	1	4
>5 and ≤10	5	12	6
>10	7	11	8
P value*	.248	<.001	

DOI, depth of invasion; T2-DOI, depth of invasion measured on coronal T2-weighted images; CET1-DOI, depth of invasion measured on coronal contrast-enhanced fat-suppressed T1-weighted images; p-DOI, depth of invasion measured on pathologic specimens.

*P value of the paired t tests comparing the values of T2-DOI with p-DOI and the values of CET1-DOI with p-DOI.

contrast-enhanced CET1-DOI adequately revealed all of the 24 lesions detectable by MRI.

Table III shows the number of cases classified by r-DOI (T2-DOI and CET1-DOI) and p-DOI. Considering the comparison between r-DOI on MRI and p-DOI (analyzed for DL patients), there was no significant difference between T2-DOI and p-DOI in univariate analysis with the paired *t* test (average 8.9 mm vs 9.9 mm, *P* = .248). The difference between T2-DOI and p-DOI was on average 1.0 mm (maximum 4.7 mm, minimum -3.3 mm). CET1-DOI values were significantly larger than p-DOI in univariate analysis with the paired *t* test (average 10.0 mm vs 6.6 mm, *P* < .001). The difference between CET1-DOI and p-DOI was on average 3.4 mm (maximum 8.8 mm, minimum -2.2 mm).

The correlation coefficient between T2-DOI and p-DOI was 0.67 (*P* = .012; Figure 6), and that between CET1-DOI and p-DOI was 0.68 (*P* < .001; Figure 7).

Interobserver agreement in the evaluation of detectability on MRI (Table IV) was very good (κ = 0.89), that of BMI (Table V) was good (κ = 0.71), and that of BFPI (Table VI) was good (κ = 0.80).

DISCUSSION

The eighth edition of the AJCC *Cancer Staging Manual* adds DOI as a tumor classification factor for oral cancer (Table I).² p-DOI has been shown to be strongly associated with neck lymph node metastasis, which is the most important prognostic factor for cancer of the

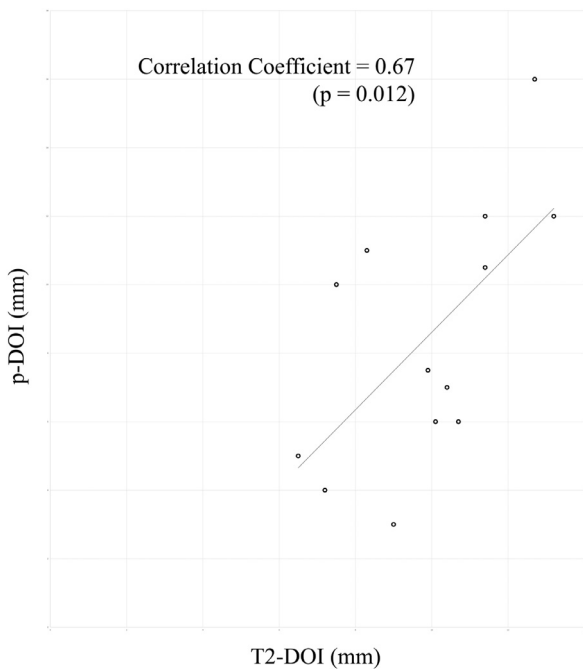


Fig. 6. Correlation between depth of invasion on coronal T2-weighted imaging and pathologic depth of invasion.

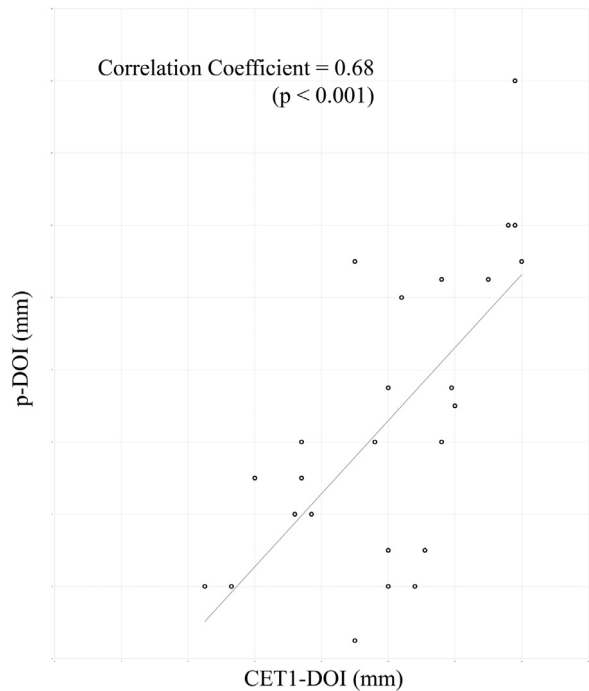


Fig. 7. Correlation between depth of invasion on coronal contrast-enhanced fat suppressed T1-weighted imaging and pathologic depth of invasion.

Table IV. Interobserver agreement on lesion detectability on MRI

		Observer 2		
		DL	UL	Total
Observer 1	DL	25	1	26
	UL	0	5	5
	Total	25	6	31

MRI, magnetic resonance imaging; DL, detectable lesions; UL, undetectable lesions.

Table V. Interobserver agreement on buccinator muscle invasion on MRI

		Observer 2		
		BMI+	BMI-	Total
Observer 1	BMI+	18	2	20
	BMI-	2	9	11
	Total	20	11	31

MRI, magnetic resonance imaging; BMI+, lesions with invasion of the buccinator muscle; BMI-, lesions without invasion of the buccinator muscle.

tongue and oral cavity.^{11,12} Lymph node metastasis is associated with a 50% reduction in 5-year survival.^{13,14} A previous study reported that p-DOI is a major predictor of neck lymph node metastasis and a determinant of

Table VI. Interobserver agreement on buccal fat pad invasion on MRI

		Observer 2		
		BFPI+	BFPI-	Total
Observer 1	BFPI+	11	3	14
	BFPI-	0	17	17
	Total	11	20	31

MRI, magnetic resonance imaging; BFPI+, lesions with invasion of the buccal fat pad; BFPI-, lesions without invasion of the buccal fat pad.

prognosis.¹⁵ The p-DOI cutoff value for determining prognosis is most commonly set at 4 mm, because a previous review demonstrated that a p-DOI greater than 4 mm strongly predicts cervical lymph node metastasis.¹⁶ Tan et al. also reported that patients with a p-DOI of 4 mm or more had higher rates of local recurrence and poorer 5-year overall survival, disease-specific survival, and local recurrence-free survival.¹⁷ Based on these studies, the National Comprehensive Cancer Network recommends neck dissection in cases with a p-DOI greater than 4 mm.¹⁸

A standard method for performing p-DOI measurement in radiologic assessment has not yet been established, and cancer staging in the *AJCC Cancer Staging Manual* suggests that DOI is difficult to estimate.² However, the results of the present investigation support the consideration of MRI-derived parameters as presurgical predictors of p-DOI. In the present study, SCCBM lesions that were not detected on MRI had a median p-DOI of 1 mm with a range of 0.5 to 3.0 mm, which means that these lesions would be classified as T1. In contrast, MRI findings of the detectable lesions with buccinator muscle invasion (BMI+) revealed a median p-DOI of 7.3 mm with a range of 0.5 to 16.0 mm, meaning that these tumors would be classified as T2 (or greater) lesions. In addition, MRI findings of the detectable lesions with buccal fat pad invasion (BFPI+) revealed a median p-DOI value of 10.5 mm with a range of 6.0 to 16.0 mm, meaning that these tumors would be classified as T2 or T3 (or greater) lesions. Previous research has demonstrated characteristic MRI findings to be useful for estimation of p-DOI.^{5,6} SCCBM that is pathologically proven but not detectable on MRI might be considered a superficial, low-volume lesion. It was reported that the p-DOI of oral tongue cancer undetected on MRI tended to be 3.5 mm or less, and 96% of the lesions had a p-DOI smaller than 4 mm.⁶ The results of the present study suggest that in carcinoma of the buccal mucosa, as in previous reports of oral tongue cancer,⁶ undetectability on MRI is thought to indicate a superficial lesion and thus is suggestive of a small DOI.

Anatomically, the styloglossus and hyoglossus muscles are located in the submucosal region of the oral tongue margin. MRI findings of styloglossus and hyoglossus invasion were confirmed in one study by the replacement of muscle tissue with a high signal intensity of tumor on T2-weighted imaging, which would normally be represented with a low signal intensity; accordingly, the p-DOI of lesions with such MRI findings tended to be greater than 7 mm.⁵ Anatomically, the buccinator muscle is present just beneath the buccal mucosa, and the buccal fat pad is deep to the buccinator muscle. The anatomic relationship of oral tongue cancer to the styloglossus and hyoglossus muscles is similar to that of carcinoma of the buccal mucosa to the buccinator muscle and buccal fat pad. In the present study, we confirmed that the p-DOI was likely to be at least 5 mm greater for BMI+ lesions (median, 7.3 mm; range, 0.5-16.0 mm) than for BMI- lesions (median, 1.5 mm; range, 0.5-4.0 mm); these differences were significant ($P < .001$). Similarly, the p-DOI was likely to be at least 6 mm larger for BFPI+ lesions (median, 10.5 mm; range, 6.0-16.0 mm) than for BFPI- lesions (median, 2.0 mm; range, 0.5-11.0 mm), also with significant differences between them ($P < .001$). These findings suggest that the presence of invasion of the buccinator muscle and/or the buccal fat pad reflects the size/volume of the tumor. In addition, consistent with previous reports of tongue cancer, BMI+ and BFPI+ lesions that were detected beneath the buccal mucosa suggest a relatively large p-DOI in carcinoma of the buccal mucosa. The actual MRI findings of detectability, BMI, and BFPI were relatively easy and clear for evaluation, with very good interobserver agreement for detectability ($\kappa = 0.89$) and good interobserver agreement for BMI and BFPI ($\kappa = 0.71$ and 0.80 , respectively).

Metastasis to cervical lymph nodes is the most important prognostic factor in oral cancer.^{11,12} The National Comprehensive Cancer Network recommends selective neck dissection in cases with a DOI greater than 4 mm, as previously mentioned.¹⁸ Therefore, the evaluation and decision for elective neck dissection in patients with N0 oral cancer is clinically important. BMI+ is more likely to have a DOI greater than 5 mm; furthermore, BFPI+ is more likely to have a DOI greater than 6 mm. Therefore, cases with MRI findings of BMI+, and especially BFPI+, should be recommended for elective neck dissection. Taken together, the results suggest that these MRI findings are valuable tools for pretreatment DOI assessment.

In the present study, 50% of the DL cases were unable to be evaluated for T2-DOI, therefore, T2-weighted images were often not useful for DOI estimation. It is possible that the normal buccal mucosa shows a high signal and thus the difficulty might be due to lack of contrast between the equally high signal of carcinoma of the buccal mucosa. However, a notable

concern is that the difference between the r-DOI and p-DOI in this study was quite heterogeneous in some cases, with the largest difference of 8.8 mm. In this case, the radiologic DOI was 10.8 mm, compared with a pathologic DOI of 2 mm, and thus it would be quite difficult to accurately assess pathologic DOI based on the radiologic DOI in such cases.

In oral tongue cancer, r-DOI on MRI has been found in previous research to correlate with p-DOI (correlation coefficient = 0.58-0.80), and r-DOI on T2-weighted imaging and contrast-enhanced T1-weighted imaging tended to be 2 to 3 mm larger than p-DOI.⁵⁻⁹ Therefore, p-DOI could be estimated by subtracting 2 to 3 mm from MRI-derived r-DOI measurements. In the present study, CET1-DOI was well correlated with p-DOI (correlation coefficient = 0.68) and, on average, the p-DOI tended to be 3.4 mm smaller than the CET1-DOI. Thus, in carcinoma of the buccal mucosa, the p-DOI might be estimated by subtracting 3.4 mm from the CET1-DOI. If evaluable, T2-DOI also correlated well with p-DOI (correlation coefficient = 0.67), which may help in p-DOI estimation. The r-DOI tends to be larger than p-DOI, possibly because of the shrinkage of specimens during formalin fixation¹⁹ and an MRI effect that increases the apparent tumor size due to adjacent inflammation and edema.²⁰ The reason for the greater difference between pathologic and imaging measurements in carcinoma of the buccal mucosa compared to tongue cancer might be that the normal buccal mucosa has a concave shape, contrary to the lingual margin. This may distort the image and make the tumor appear thicker (and thus result in a larger r-DOI) because it is shaped to envelop the carcinoma. However, the reasons for these details are unclear.

Ultrasonography can also aid in assessing tumor extent and DOI. A very strong correlation has been reported between DOI on ultrasound images and p-DOI of oral cancer (correlation coefficient = 0.867).²¹ Ultrasonography has some disadvantages, such as operator-dependent image quality and images that are less objective than those of computed tomography and MRI. However, the usefulness of ultrasound is apparent owing to its high correlation coefficient, its ability to be performed intraoperatively and immediately before surgery, and its ability to identify epithelial dysplasia. It is anticipated that future studies will be aimed at systematic accumulation of cases and research on the usefulness of ultrasonography for diagnosing depth of carcinoma in the buccal mucosa.

There were several limitations to our study. The study was retrospective, included a small number of patients, and involved a single center. Larger studies would be needed to confirm our results.

CONCLUSION

MRI-derived parameters of SCCBM can be helpful in estimating the pathologic depth of invasion of these tumors. Undetectability of lesions on MRI could suggest a p-DOI equivalent to T1, with low risk of metastasis. Significant differences in p-DOI between lesions that invade the buccinator muscle and/or buccal fat pad and noninvasive lesions indicate that invasion suggests a p-DOI that would classify the lesion as T2 or greater. Measurement of r-DOI on CET1 images correlated well with p-DOI and were generally a few millimeters larger than the actual pathologic depth. This may prove helpful in estimating the p-DOI presurgically and subsequently determining the necessity of elective neck dissection.

ACKNOWLEDGMENT

We are grateful of Dr. Reina Kayama for editing parts of this article.

REFERENCES

1. Japan Society for Head and Neck Cancer Cancer Registry Committee. Report of head and neck cancer registry of japan clinical statistics of registered patients, 2016. http://square.umin.ac.jp/jshnc/pdf/2016syousei_houkoku.pdf.
2. Amin MB, Edge S, Greene FL, et al, eds. *AJCC Cancer Staging Manual*, 8th ed., New York: Springer; 2017. <https://doi.org/10.3322/caac.21388>.
3. den Toom IJ, Janssen LM, van Es RJJ, et al. Depth of invasion in patients with early stage oral cancer staged by sentinel node biopsy. *Head Neck*. 2019;41:2100-2106.
4. Ahmed SQ, Junaid M, Awan S, et al. Relationship of tumor thickness with neck node metastasis in buccal squamous cell carcinoma: an experience at a tertiary care hospital. *Int Arch Otorhinolaryngol*. 2017;21:265-269.
5. Baba A, Okuyama Y, Yamauchi H, et al. Magnetic resonance imaging findings of styloglossus and hyoglossus muscle invasion: relationship to depth of invasion and clinical significance as a predictor of advisability of elective neck dissection in node negative oral tongue cancer. *Eur J Radiol*. 2019;118:19-24.
6. Baba A, Okuyama Y, Ikeda K, et al. Undetectability of oral tongue cancer on magnetic resonance imaging; clinical significance as a predictor to avoid unnecessary elective neck dissection in node negative patients. *Dentomaxillofacial Radiol*. 2019;48:1-6.
7. Baba A, Ojiri H, Ogane S, et al. Usefulness of contrast-enhanced CT in the evaluation of depth of invasion in oral tongue squamous cell carcinoma: comparison with MRI. *Oral Radiol*. 2021;37:86-94.
8. Murakami R, Shiraishi S, Yoshida R, et al. Reliability of MRI-derived depth of invasion of oral tongue cancer. *Acad Radiol*. 2019;26:e180-e186.
9. Mao M-H, Wang S, Feng Z, et al. Accuracy of magnetic resonance imaging in evaluating the depth of invasion of tongue cancer. A prospective cohort study. *Oral Oncol*. 2019;91:79-84.
10. Landis JR, Koch GG. The measurement of observer agreement for categorical data. *Biometrics*. 1977;33:159-174.
11. Iwai H, Kyomoto R, Ha-Kawa SK, et al. Magnetic resonance determination of tumor thickness as predictive factor of cervical metastasis in oral tongue carcinoma. *Laryngoscope*. 2002;112:457-461.
12. Layland MK, Sessions DG, Lenox J. The influence of lymph node metastasis in the treatment of squamous cell carcinoma of the oral cavity, oropharynx, larynx, and hypopharynx: N0 versus N+. *Laryngoscope*. 2005;115:629-639.

13. Snow GB, Annys AA, Eavan Slooten, et al. Prognostic factors of neck node metastasis. *Clin Otolaryngol Allied Sci.* 1982;7:185-192.
14. Grandi C, Alloisio M, Moglia D, et al. Prognostic significance of lymphatic spread in head and neck carcinomas: therapeutic implications. *Head Neck Surg.* 1985;8:67-73.
15. Patel RS, Clark JR, Dirven R, et al. Prognostic factors in the surgical treatment of patients with oral carcinoma. *ANZ J Surg.* 2009;79:19-22.
16. Huang SH, Hwang D, Lockwood G, et al. Predictive value of tumor thickness for cervical lymph-node involvement in squamous cell carcinoma of the oral cavity. *Cancer.* 2009;115:1489-1497.
17. Tan WJ, Chia CS, Tan HK, et al. Prognostic significance of invasion depth in oral tongue squamous cell carcinoma. *ORL J Otorhinolaryngol Relat Spec.* 2012;74:264-270.
18. Pfister DG, Spencer S, Adelstein D, et al. NCCN clinical practice guidelines in oncology head and neck cancers v.2. https://www.nccn.org/professionals/physician_gls/pdf/head-and-neck.pdf. Accessed August 31, 2020.
19. Johnson RE, Sigman JD, Funk GF, et al. Quantification of surgical margin shrinkage in the oral cavity. *Head Neck.* 1997;19:281-286.
20. Lam P, Au-Yeung KM, Cheng PW, et al. Correlating MRI and histologic tumor thickness in the assessment of oral tongue cancer. *Am J Roentgenol.* 2004;182:803-808.
21. Iida Y, Kamijo T, Kusafuka K, et al. Depth of invasion in superficial oral tongue carcinoma quantified using intraoral ultrasonography. *Laryngoscope.* 2018;128:2778-2782.
22. Baba Akira, Hashimoto Kazuhiko, Kayama Reina, et al. Radiological approach for the newly incorporated T staging factor, depth of invasion (DOI), of the oral tongue cancer in the 8th edition of American Joint Committee on Cancer (AJCC) staging manual: assessment of the necessity for elective neck dissection. *Japanese Journal of Radiology.* 2020;38(9):821-832. <https://doi.org/10.1007/s11604-020-00982-w>.

Reprint requests:

Akira Baba, MD, PhD
Department of Radiology
The Jikei University School of Medicine
3-25-8 Nishi-Shimbashi
Minato-ku
Tokyo 105-8461
Japan.
akirababa@jikei.ac.jp